Optical spectroscopy of tungsten carbide (WC)

Shane M. Sickafoose, Adam W. Smith, and Michael D. Morse
Department of Chemistry, University of Utah, Salt Lake City, Utah 84112

(Received 27 August 2001; accepted 19 October 2001)

Resonant two-photon ionization spectroscopy has been used to study the diatomic transition-metal carbide, WC. A low-resolution scan revealed a five-member vibrational progression beginning with the 0-0 band at 17 585 cm^{-1}. Analysis of this progression yielded a vibrational frequency of $\omega_e'(^{184}W^{12}C) = 752.6(4.9)\ cm^{-1}$ and a bond length of $r_e'(^{184}W^{12}C) = 1.747(4)$ Å. Several unassigned bands were also rotationally resolved and analyzed. All of the observed bands are $\Omega' = 2 \leftarrow \Omega'' = 1$ transitions, confirming the predicted ground state of $^3\Delta_1$ arising from a $14\sigma^2 8\pi^4 15\sigma^2 4\delta^1 16\sigma^1$ configuration. The measured line positions in these bands were simultaneously fitted to provide $B_0'' = 0.509\,66(10)\ cm^{-1}$ for $^{184}W^{12}C$, corresponding to $r_0''(^{184}W^{12}C) = 1.713\,5(2)$ Å. These values are corrected for spin-uncoupling effects in the ground state and represent our best estimate of the true bond length of WC. Dispersed fluorescence studies provide the ground-state vibrational constants of $\omega_e = 983(4)\ cm^{-1}$ and $\omega_e x_e = 11(1)\ cm^{-1}$, and have also permitted the low-lying $[1.2]\,^3\Delta_2$ and [4.75] states to be located and characterized. These results on WC are discussed in relation to the isovalent molecule MoC and other transition-metal carbides. © *2002 American Institute of Physics.* [DOI: 10.1063/1.1427068]

I. INTRODUCTION

The interaction between transition metals and organic molecules is the basis for many catalytic processes useful to organic chemistry and to the chemical industry.[1] A large number of transition-metal complexes have been developed to increase the rates and enhance the selectivity of important synthetic organic reactions.[2–4] Many of these reactions depend on the formation, rearrangement, and subsequent breaking of a metal–carbon bond, so experimental characterization of the bond between the transition-metal atom and carbon is important for achieving a full understanding of these systems. To further this end, we have embarked on a study of the diatomic transition-metal carbides, and have already reported on the electronic spectroscopy and electronic structure of FeC,[5] MoC,[6,7] RuC,[7,8] and PdC.[7,9] In this paper we extend these studies to the 5*d* transition-metal series by reporting on the electronic spectroscopy of WC.

Prior to the development of laser ablation sources, relatively few transition-metal monocarbides were spectroscopically investigated. The earliest studies include optical studies and Knudsen effusion studies on RuC,[10–12] RhC,[13–16] IrC,[12,17,18] and PtC.[16,19–22] Since the invention of the laser ablation source, many more transition-metal monocarbides have been interrogated.[5,6,8,9,23–37] The 4*d* transition-metal monocarbides have been rather thoroughly investigated,[6,8,9,27–32] with TcC, AgC, and CdC being the only members of this class that remain spectroscopically unexamined. Recent articles from this group examine the trends in the chemical bonding and electronic structure as the 4*d* series of transition-metal monocarbides is traversed.[6,7]

The 3*d* transition-metal monocarbides have also undergone a significant number of experimental and theoretical inquiries. Published spectroscopic analyses exist for FeC (Refs. 5, 38, and 39) and CoC (Refs. 25, 26, and 40), and two papers are currently in preparation from this group on NiC.[41,42] In addition, rotationally resolved spectra of TiC and CrC have been recorded in our laboratory, but these have not yet been successfully analyzed. Preliminary data has also been collected on VC in our laboratory. Electron spin resonance spectra have been reported for matrix-isolated VC,[40,43] and theoretical investigations have been reported for TiC,[44–46] VC,[47,48] CrC,[49,50] FeC,[51] and NiC.[52,53]

In contrast, rather little is known about the 5*d* transition-metal monocarbides. Previous experimental studies have focused on PtC (Refs. 34–37 and 54) and IrC (Refs. 33 and 54), and these molecules are now well characterized. For most of the remaining 5*d* transition-metal monocarbides, Knudsen effusion mass spectrometric measurements of the bond energy provide the only experimental data. Theoretical calculations have been reported for TaC (Ref. 55) and IrC (Ref. 56), and ReC has undergone a preliminary investigation in this group, with many vibronic transitions found above 17 700 cm^{-1}.

Tungsten carbide has recently been the focus of two investigations. A photoelectron spectroscopy (PES) study of mass-selected WC^- by Wang and co-workers assigned the ground state as $^3\Delta_1$ and located several excited electronic states lying below 19 400 cm^{-1}.[30] Balasubramanian then performed complete active space multiconfiguration self-consistent field (CASSCF) calculations on WC, followed by full first- and second-order configuration-interaction calculations that included spin–orbit effects via a relativistic configuration-interaction (RCI) method.[57] These calculations agreed with the assignment of a $^3\Delta_1$ ground state, but suggested that some of the states assigned in the PES study should be reassigned. Other recent studies on small tungsten molecules include matrix isolation studies of WN (Ref. 58) and rotationally resolved gas-phase work on WN (Ref. 59) and WCH (Ref. 60).

The present study is the first investigation of diatomic WC by optical spectroscopic methods and provides the first rotationally resolved studies of this molecule. The dispersed fluorescence work reported here likewise provides the first experimental information concerning the vibrational levels for any electronic state of this molecule. In the next section we briefly describe the experimental techniques employed to study WC. Section III presents the spectra that have been collected and describes their interpretation, including fitting of the rotational lines and the identification and fitting of vibrational progressions. Section IV compares the present results with the results from the two previous investigations of WC, and notes the differences between the electronic structure of WC and MoC, which we have investigated previously. A summary of our most important conclusions is then presented in Sec. V.

II. EXPERIMENT

A complete description of the resonant two-photon ionization (R2PI) spectrometer and the experimental procedure can be found in earlier publications,[61,62] so only a brief description is presented here. The molecular source consists of a 1/8-in.-diam tungsten rod (Alfa Aesar, 99.95%), which is subjected to the focused output of a frequency-doubled neodymium-doped yttrium aluminum garnet (Nd:YAG) laser pulse (Quantel, 532 nm, 3 mJ/pulse). This ablates metal atoms from the rod surface, forming a metal plasma that is entrained in a helium carrier gas pulse containing 3% methane. The methane and hot metal atoms react to form a variety of products as they travel down a 4-mm-long channel before undergoing supersonic expansion into vacuum via a 2-mm-diam orifice. Through optimization of the on-resonance signal of WC, the optimal backing pressure for the gas reservoir was determined to be 2–3 PSIG (pounds per square inch gauge). The molecular jet was skimmed to a 5-mm-diam beam prior to entering the Wiley–McLaren extraction region[63] of a differentially pumped reflectron time-of-flight mass spectrometer.[64] Resonant two-photon ionization spectroscopy was performed by exposing the molecules to two sequential laser pulses. The excitation laser pulse was generated by a tunable dye laser (Molectron DL-II) pumped by either the frequency-doubled or tripled output of a Nd:YAG laser (Quantel, 581-C). The ionization laser pulse was the output of an ArF excimer laser (Lambda Physik, Compex 201) at 6.42 eV.

The diffraction grating housed in the dye laser provided radiation with a linewidth of 0.6 cm^{-1}, sufficiently narrow to identify discrete vibronic transitions. For rotational analysis of each band, however, an air-spaced étalon was introduced into the oscillator cavity, which was then pressure tuned over a range of 6–8 cm^{-1} using sulfur hexafluoride (SF_6). This process produced radiation with a laser linewidth of 0.03 cm^{-1}.

Calibration of the radiation generated for rotationally resolved scans was accomplished through the simultaneous collection of an I_2 laser-induced fluorescence (LIF) spectrum for transitions below 20 000 cm^{-1}. The LIF spectrum was then compared to the atlas of Gerstenkorn and Luc for absolute calibration.[65] For transitions above 20 000 cm^{-1}, isotopically pure ^{130}Te was heated to either 510 or 650 °C, and an absorption spectrum of $^{130}Te_2$ was collected and compared to the atlas of Cariou and Luc.[66] The calibrated molecular spectra were then corrected for the Doppler shift due to the velocity of the molecular beam relative to the excitation laser radiation. The measured line positions are believed to have an absolute accuracy of ± 0.02 cm^{-1}.

The instrument used for the dispersed fluorescence of WC has been described in earlier studies reported by this group,[7] and the molecular source was identical to that of the R2PI experiment described above. The tunable dye laser system used in the R2PI experiment described above was also used to excite transitions in WC for dispersed fluorescence studies. The induced fluorescence was collected perpendicular to both the molecular beam and the incident excitation laser beam, and then was imaged onto the 100-μm-wide slit of a spectrograph (Acton Research Corp., Acton, MA; 500-mm focal length, f/6.5). Inside the spectrograph, the radiation was dispersed with one of three available diffraction gratings (300 lines/mm, 500-nm blaze; 1800 lines/mm, 500-nm blaze; or 2400 lines/mm, holographic), and was imaged onto the head of the gated, intensified charge-coupled device (CCD) camera (Roper Scientific, Trenton, NJ). The spectra were calibrated using known Hg, Ar, and Ne atomic lines emitted from hollow cathode tubes, as reported in the MIT wavelength tables.[67]

To reduce the extraneous signal originating from glowing metal particles that pass below the collection optics, the microchannel plate on the intensifier head of the CCD was gated in time using a commercially obtained pulse generator (PG-10, Roper Scientific, Trenton, NJ). The much heavier particles tend to pass through the imaged region at least 50 μs after the diatomic molecules. Setting the gate pulse width to 1 μs reduced the radiation originating from other sources, allowing a gross differentiation between sizes of molecular species.

III. RESULTS

A. Resonant two-photon ionization spectra

A potential difficulty in spectroscopic investigations of the transition-metal monocarbides is the possibility of misidentification of transitions belonging to molecular species

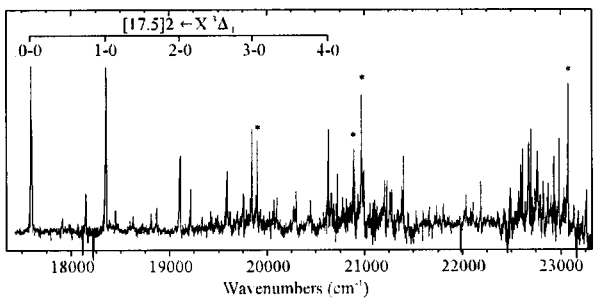

FIG. 1. Resonant two-photon ionization spectrum of WC, over the range from 17 500 to 23 250 cm^{-1}. The v'-0 bands of the $[17.6]2 \leftarrow X\,^3\Delta_1$ band system are labeled. All five of the members of this system were rotationally resolved. Bands indicated by an asterisk were also rotationally resolved in this investigation.

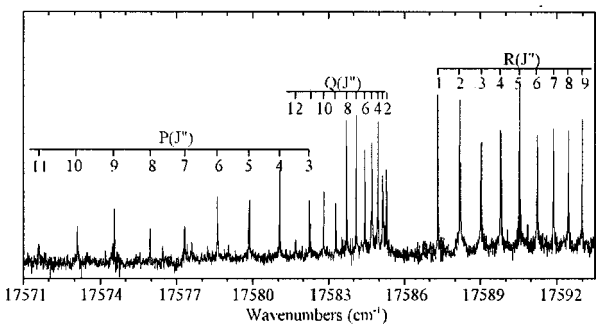

FIG. 2. Rotationally resolved scan over the 0-0 band of the $[17.6]2 \leftarrow X\,^3\Delta_1$ system of $^{184}W^{12}C$. The first lines $R(1)$, $Q(2)$, and $P(3)$ prove that this is an $\Omega'=2 \leftarrow \Omega''=1$ transition.

other than the molecule of interest. It is an advantage to use a mass-resolved technique such as R2PI spectroscopy, but misidentification is still possible. The four abundant isotopes of tungsten (^{182}W, 26.3%; ^{183}W, 14.3%; ^{184}W, 30.1%; ^{186}W, 28.6%) provided a distinctive set of mass peaks useful for identifying tungsten-containing species. The tungsten monocarbide mass peaks, however, are only 1 amu below the previously studied tungsten methylidyne, WCH.[60] The mass spectra of the two species overlap, but $^{182}W^{12}C$, $^{186}W^{12}C$, ^{184}WCH, and ^{186}WCH possess masses unique to their particular molecule. The ion signal from tungsten methylidyne on resonance was originally used to optimize the source for production of small tungsten-bearing molecules, but careful use of a well-calibrated mass spectrometer prevented any confusion as to which molecular species was on resonance for each transition. The bands reported in this paper are due solely to tungsten monocarbide.

1. General features

In low-resolution scans of the spectral region from 17 000 to 23 100 cm^{-1}, more than 15 discrete bands were found, as displayed in Fig. 1. Of these bands, 9 were deemed intense enough for rotational analysis.

All of the rotationally resolved bands exhibited the same general appearance of a strong Q branch with a stronger R branch and a weak P branch, implying an electronic transition with $\Delta\Omega=+1$.[68] A typical spectrum is displayed in Fig. 2. The rotational lines were fitted by assigning each line an integer J'' value and a branch assignment. The lines were then fitted using the standard equation[68]

$$\nu=\nu_0+B'J'(J'+1)-B''J''(J''+1). \tag{3.1}$$

For all of the rotationally resolved bands, the R branch begins with $J''=1$ and continues to higher J values, with the spacing between the rotational lines decreasing until reaching a band head. The Q branch begins with $J''=2$. The Q lines are almost as intense as the R branch and continue out to lower wave numbers with increasing spacing between the rotational lines. The first line in the P branch is $P(3)$ and all of the P lines are much less intense than either the R lines or the Q lines. In many of the rotationally resolved bands, the decrease in the spacing between the R branch lines led to a band head value of J'' sufficiently low to be observed. This indicates a significant increase in bond length upon electronic excitation, as is borne out by detailed analysis of the spectra.

The rotationally resolved bands were fitted individually to Eq. (3.1), and all had first lines of $R(1)$, $Q(2)$, and $P(3)$, indicating that the bands are $\Omega'=2 \leftarrow \Omega''=1$ transitions. The fitted B'' values were identical for all of the bands, within the 1σ error limits, implying that all of the bands originated from the same lower state. This observation permitted all of the rotationally resolved bands, except for the two bands contained in the single feature near 19 100 cm^{-1}, to be fitted simultaneously. The reason for the removal of these bands will be discussed in the following subsection. The simultaneous fit produced the best possible value for the lower-state rotational constant. A summary of the results from this simultaneous fit is provided for the most abundant isotopomer, $^{184}W^{12}C$, in Table I. A complete listing of the fitted rotational lines, along with the fitted parameters ν_0, B', and B'', for $^{182}W^{12}C$, $^{183}W^{12}C$, $^{184}W^{12}C$, and $^{186}W^{12}C$ is available through EPAPS[69] or from the author (M.D.M.).

The fitted value of B'' for $^{184}W^{12}C$ is 0.509 22(10) cm^{-1}, but this is merely the effective B value for this state. It is well known that the measured B_{eff} values for Hund's case (a) multiplet states are related to the true, mechanical B value by the formula[70]

$$B_{\text{eff}}=B\left(1+\frac{2B\Sigma}{A\Lambda}\right), \tag{3.2}$$

where $A\Lambda$ is the spin–orbit splitting and Σ is the projection of electron spin on the internuclear axis. Setting $A\Lambda$ equal to the energy difference between the $X\,^3\Delta_1$ ground state and the $[1.2]\,^3\Delta_2$ excited spin–orbit level, which was measured in dispersed fluorescence experiments described below to be 1188 cm^{-1}, Eq. (3.2) may be used to convert the measured B_{eff} value to the true, mechanical B value for this system. This leads to a modest correction, giving $B_0''=0.509\,66(10)$ cm^{-1} as compared to the effective B value of 0.509 22(10) cm^{-1}. Inverting this value to obtain the bond length, a value of $r_0''=1.7135(2)$ Å is obtained.

2. The $[17.6]2 \leftarrow X\,^3\Delta_1$ system

The band near 17 585 cm^{-1} is the first of a five-member progression showing a rather even vibrational spacing. The assignment of the 17 585-cm^{-1} band as a 0-0 band is based on the small isotope shift, defined as $\Delta\nu_0=\nu_0(^{182}WC)-\nu_0(^{186}WC)$, of 0.0198 cm^{-1}. The lack of other intense bands between most members of the progression made assignment relatively straightforward. The bands march out to higher energy with a relatively even spacing, as expected. To identify the upper state of this band system in a unique way, we refer to it as the [17.6]2 state, where the energy of the $v=0$ level, in thousands of cm^{-1}, is given in square brackets while the Ω value of the state is provided after the square brackets.

In general, the isotope shift, $\Delta\nu_0$, is expected to increase in a nearly linear fashion as the vibrational quantum number of the upper state increases. This property of the isotope shift was used to distinguish which of the two features near 19 850 cm^{-1} is the $v'=3 \leftarrow v''=0$ transition. The band at

TABLE I. Fitted parameters of $^{184}W^{12}C$.[a]

B''	ν_0	B'	H_{12}	$\Delta\nu_0$[b]	τ (μs)	r (Å)
0.509 22(10)						1.7143(2)
	17 585.4233(22)	0.485 36(6)		0.0198	0.483(16)	1.7559(1)
	18 343.2957(24)	0.482 09(5)		0.5223	0.396(7)	1.7618(1)
	19 096.832(53)	*0.445 82(157)*	*2.09(3)*	*1.332*	*0.656(32)*	*1.8321(32)*
	19 095.230(47)	*0.472 91(96)*		*0.665*		*1.7789(18)*
	19 835.6591(54)	0.445 78(10)		0.9421	0.846(138)	1.8322(2)
	19 889.7739(34)	0.429 59(9)		0.3356	1.641(133)	1.8664(2)
	20 615.6634(57)	0.458 45(16)		1.1503	0.680(10)	1.8067(3)
	20 881.7961(85)	0.443 99(17)		1.1785	1.848(71)	1.8359(4)
	20 955.6496(36)	0.450 20(11)		1.5615		1.8232(2)
	20 962.2638(31)	0.426 44(11)		0.9266		1.8733(2)
	20 963.5225(41)	0.441 12(42)		2.5120		1.8418(9)
	23 061.9830(90)	0.438 08(24)		1.4268		1.8482(5)

[a]All numerical values are given in wave numbers (cm^{-1}), except for τ values, which are in units of microseconds (μs), and r_0'' values, which are in units of ångströms (Å). The 1 σ errors are given in parentheses in units of the last decimal quoted. The reported B values, along with the derived r values, are effective parameters that have not been corrected for **L** and **S**-uncoupling interactions with nearby states. When a correction for the **S**-uncoupling interaction is made for the ground $X\,^3\Delta_1$ state, as described in the text, corrected values of $B_0''=0.50966(10)$ cm^{-1} and $r_0''=1.7135(2)$ Å are obtained. Italicized values are obtained following the deperturbation procedure described in Section III.A.2.

[b]$\Delta\nu_0$ provides the isotope shift of the band, defined as $\Delta\nu_0=\nu_0(^{182}W^{12}C)-\nu_0(^{186}W^{12}C)$.

19 890 cm^{-1} has an isotope shift of 0.3356 cm^{-1}, which is much less than the isotope shift of the band at 19 836 cm^{-1} (0.9421 cm^{-1}) and also less than the shift measured for the $1\leftarrow0$ band at 18 343 cm^{-1} (0.5223 cm^{-1}). These facts strongly suggest that the band at 19 836 cm^{-1} should be assigned as the $3\leftarrow0$ band. Additional evidence in favor of this assignment is the fact that both the B' value and the upper-state lifetime of this band are more consistent with the other members of the progression than are the corresponding values for the 19 890-cm^{-1} band. Nevertheless, it is troubling that the B' value for this band is significantly smaller than those of the other members of the progression. Likewise, the upper-state lifetime of this band is significantly longer than that of the remaining members of this band system. We believe that these discrepancies result from a perturbation between the upper states of the 19 836 and 19 890 cm^{-1} bands.

The feature near 19 100 cm^{-1} appeared to be a single feature in low resolution, but when rotationally resolved, two $\Omega'=2\leftarrow\Omega''=1$ bands were revealed with intermingled rotational lines. The rotational lines of these two bands were sorted out, and each band was fitted independently following Eq. (3.1). The residuals in the resulting fits were much larger than expected given the laser bandwidth and were unacceptable. Systematic trends in the residuals suggested that the two upper states were perturbing one another, and a two-state deperturbation analysis was attempted in order to obtain a valid fit.

The method of Langenberg, Shao, and Morse[9] was followed for this deperturbation analysis. The total energy of each upper-state rotational level was calculated by adding the ground-state rotational energy to the measured wave number. The rotational energy of the ground state was calculated using the value of B'' obtained from the simultaneous fit of the other bands by employing the equation $F''(J'')=B''J''(J''+1)$. This value was then added to the measured wave number. When more than one line terminated in the same J' level, the calculated upper-state energies were averaged. The resulting energies of the upper and lower members of the perturbing pair of states, designated as $E^+(J)$ and $E^-(J)$, were assumed to be the solutions of a two-state perturbation model in which the Hamiltonian matrix is given as

$$\underline{\underline{H}}=\begin{pmatrix} T^+ + B^+J(J+1) & H_{12} \\ H_{12} & T^- + B^-J(J+1) \end{pmatrix}. \tag{3.3}$$

In this equation, $T^{\pm}$ and $B^{\pm}$ are the term energy and rotational constant for the upper and lower members of the perturbing pair of states, respectively. The perturbation matrix element H_{12} is assumed to be constant over the range of rotational levels observed in our experiments, as is expected for the interaction between two states with the same value of Ω. The upper and lower energy levels were then fitted simultaneously using the equations

$$E^+(J)=\tfrac{1}{2}((T^++T^-)+(B^++B^-)J(J+1) + \{[(T^+-T^-)+(B^+-B^-)J(J+1)]^2+4H_{12}^2\}^{1/2}) \tag{3.4}$$

and

$$E^-(J)=\tfrac{1}{2}((T^++T^-)+(B^++B^-)J(J+1) - \{[(T^+-T^-)+(B^+-B^-)J(J+1)]^2+4H_{12}^2\}^{1/2}). \tag{3.5}$$

In the fitting routine, $T^{\pm}$, $B^{\pm}$, and H_{12} were varied to obtain the best fit in a nonlinear least-squares procedure.

The residuals obtained using this fitting procedure were much more reasonable and produced rotational constants nearer to the expected values. Once these bands were fitted, it was a simple matter to determine which deperturbed state was the $v'=2$ level of the observed progression and which was the interloper by their deperturbed isotope shifts and rotational constants. The higher-frequency band has an iso-

TABLE II. Fitted ν_0 and B_v' values for the [17.6]2 state of $^{184}W^{12}C$.[a]

$v' \leftarrow v''$	Measured ν_0		Measured B_v'
0←0	17 585.423(−0.938)		0.485 36(−158)
1←0	18 343.296(0.250)		0.482 09(214)
2←0	19 095.230(−1.875)		0.472 91(−43)
3←0	19 835.7[−19.6]		0.445 78[−2018]
4←0	20 615.664(0.313)		0.458 45(−51)
	Fitted parameters		
T_0	17 586.361(3.141)	B_e'	0.490 44(200)
ω_e'	752.559(4.882)	α_e'	0.006 99(117)
$\omega_e' x_e'$	−0.938(0.925)	r_e'	1.747(4)

[a]All numerical values are given in wave numbers (cm^{-1}), except for r_e', which is given in ångströms (Å). Residuals in the fit are given in parentheses following the values of ν_0 and B_v' in units of cm^{-1}. Because the $v' = 3$ level is perturbed, it has been omitted from the fit. The values in square brackets [ ] provide the difference between the measured value and the value predicted using the fit results for the 3-0 band.

tope shift of 1.332 cm^{-1}, while the lower-frequency band has an isotope shift of 0.665 cm^{-1}, much more in line with the isotope shifts measured for other members of the progression. Similarly, the B' value of the lower of the two deperturbed states was clearly in line with the B' values of the $v' = 0$ and $v' = 1$ levels.

The identification of the 2-0 band completed the assignment of the observed vibrational progression and permitted the progression to be fit using[71]

$$\nu_0(v'\text{-}0) = T_0 + v'\omega_e - (v'^2 + v')\omega_e x_e, \tag{3.6}$$

where $\nu_0(v'\text{-}0)$ is the band origin of the v'-0 band, determined from the fit of the rotational lines, T_0 is the wave number of the 0-0 band, ω_e and $\omega_e x_e$ are the vibrational frequency and anharmonicity of the excited electronic state, and v' is the upper-state vibrational quantum number. In the fit of the vibrational levels to Eq. (3.6), the 3←0 band was excluded, because inclusion of this data point led to a large residual in the fit. This, along with other indications that are discussed below, lead us to believe that the $v' = 3$ level is perturbed. Excluding the $v' = 3$ level, a reasonable fit is obtained. The fitted data and parameters for the [17.6]2 $\leftarrow X(\Omega'' = 1)$ band system are compiled in Table II.

For all of the isotopomers, the calculated wave number of the 3←0 band is approximately 20 cm^{-1} above the measured value. This shift is indicative of a perturbing state at higher energy. Presumably, the perturbing state is the upper level of the transition observed at 19 890 cm^{-1}. These two states are approximately 55 cm^{-1} apart, which is too large to observe measurable deviations from the $BJ(J+1)$ form normally expected for the rotational levels. This precludes us from attempting to deperturb these bands, since a departure from the $BJ(J+1)$ form is needed to obtain information about the magnitude of the interaction.

Additional evidence of a perturbation in the $v' = 3$ level is found when the measured rotational constants are fitted to the standard formula[71]

$$B_v = B_e - \alpha_e(v + \tfrac{1}{2}) \tag{3.7}$$

to extract the equilibrium rotational constant B_e and the vibration–rotation interaction constant α_e. Including the $v' = 3$ level in the fit leads to an unacceptably large residual, as is obvious from the fact that B_3' is smaller than B_4'. Omitting the $v' = 3$ level from the fit again leads to a generally acceptable fit that allows r_e' to be determined as 1.747(4) Å. The fit of the rotational constants to Eq. (3.7) is also presented in Table II.

3. Unassigned resolved bands

The assignment of five bands to a vibrational progression still leaves four bands unassigned. The bands at 19 890, 20 882, and 23 062 cm^{-1} all exhibit the same rotational structure, as do the bands assigned to the vibrational progression. These bands also have first lines of $R(1)$, $Q(2)$, and $P(3)$ and are therefore $\Omega' = 2 \leftarrow X(\Omega'' = 1)$ transitions.

The last of the bands that was rotationally resolved lies near 20 960 cm^{-1}. The feature seen in low resolution appears to be a single, reasonably strong transition. The rotationally resolved spectrum, however, does not display the simple R, Q, P branch structure that was found for the other bands. Instead, an initially bewildering array of rotational lines was observed. Because the ground-state rotational constant had already been determined, however, it was possible to sort out sets of rotational lines using the combination difference method.[68] This method is based on the fact that rotational lines terminating on the same upper level are separated by an amount that depends only on the ground-state rotational constant. For lines terminating on the upper state labeled by J, this gives

$$R(J-1) - Q(J) = 2B''J, \tag{3.8}$$

$$Q(J) - P(J+1) = 2B''(J+1), \tag{3.9}$$

and

$$R(J-1) - P(J+1) = 2B''(2J+1). \tag{3.10}$$

Because B'' is well-determined from the fit of the other bands, we were able to search the spectrum for lines separated by the multiples of $2B''$ listed above. This procedure allowed the observed rotational lines to be clearly identified. This analysis revealed the presence of three separate bands occurring within 10 cm^{-1} of each other. Surprisingly, the rotational lines of each band gave small residuals when the measured line positions were fit according to Eq. (3.1). This implies that these three upper states do not perturb each other within the limits of the resolution of our experiment. All three of the bands fit with lowest lines of $R(1)$, $Q(2)$, and $P(3)$, indicating that they also are $\Omega' = 2 \leftarrow X(\Omega'' = 1)$ transitions. All six of these unassigned bands were included in the final simultaneous fit to determine the rotational constant of the ground state.

B. Dispersed fluorescence spectra

In any spectroscopic investigation involving an impure sample, there is concern that the molecular source of the signal may be misidentified. In dispersed fluorescence studies, this concern is more acute because there is no direct method, such as separation of species by mass, that can be used to isolate the spectrum of the molecule of interest from that of other molecules. Therefore, procedures must be fol-

TABLE III. WC bands excited and the resulting levels observed by dispersed fluorescence.

Band excited			Levels observed		
Band system	ν_0 (cm^{-1})	v'-v''	$X\,^3\Delta_1$	$[1.2]\,^3\Delta_2$	[4.75]
$[17.6]2\leftarrow X\,^3\Delta_1$	17 584.32	0-0	0,1	0,1	
	18 341.42	1-0	0–3	0,1	
	19 091.57	2-0	0,1,2		
	19 828.08	3-0	0–3	1,2	
	19 875.99	4-0	0–3		0
Unassigned bands	20 608.79		0–3	2	0
	20 861.50		0–3		0,1
	20 951.11		0,2,3		

lowed to ensure that the dispersed fluorescence signal truly originates from the molecule of interest. To this end, the excitation frequencies employed for dispersed fluorescence were selected from strong vibronic transitions found during the R2PI study of WC. Because the same laser was used in both experiments, tuning up on a transition was as trivial as setting the dye laser to the wavelength where the transition was first found. While it is possible that other molecules present in the molecular beam might have transitions that coincide with these resonant frequencies, it is unlikely that they would resonate through more than one of the eight excitation frequencies explored in this study. Therefore, we feel confident that the dispersed fluorescence spectra described below truly do represent fluorescence spectra of WC.

1. General features

To analyze the low-energy states of WC, dispersed fluorescence spectra were collected from 8 of the 15 bands found in the R2PI study. Fluorescence to the ground state and to two additional low-lying electronic states was observed. Dispersed fluorescence spectra were first collected using the 300-lines/mm diffraction grating. For fluorescence bands having sufficient intensity, higher-resolution spectra were recorded using either the 1800- or 2400-lines/mm grating. While the resolution of the experiment (1.5–5 cm^{-1}) was not sufficient to resolve the individual rotational lines, a contour of the rotational features could be observed. When sufficient intensity was available for these higher-resolution measurements, comparison of the relative intensities of the *P*, *Q*, and *R* branches to the predictions of the Hönl–London formulas allowed us to determine the $\Delta\Omega$ value for the emission.[68]

Table III lists the excitations employed and fluorescence bands observed for WC. The energy of the lower state of each fluorescence band was determined by placing the observed fluorescence bands on a common energy scale using $\nu_{\rm rel}=\nu_{\rm ex}-\nu_{\rm em}$, where $\nu_{\rm ex}$ and $\nu_{\rm em}$ are the excitation and emission wave numbers, respectively. To decrease the experimental uncertainty in each measured energy level, the relative wave numbers for each multiply observed level were averaged, and the resulting energy levels were fitted to Eq. (3.6). Table IV lists the assigned vibronic levels measured by dispersed fluorescence, their measured energies, and the spectroscopic constants corresponding to each of the observed states.

TABLE IV. Vibronic levels of low-lying states of WC and fitted spectroscopic constants.[a]

Electronic state	v	Energy (cm^{-1})	Fitted energy (cm^{-1})	Residual (cm^{-1})
$X\,^3\Delta_1$	0	0.0	0.0	0.0[b]
	1	959.82	961.54	−1.72
	2	1903.10	1901.38	1.72
	3	2818.97	2819.54	−0.57
$[1.2]\,^3\Delta_2$	0	1188.66	1188.66	0.0[c]
	1	2167.86	2167.86	0.0[c]
	2	3123.60	3123.60	0.0[c]
[4.75]	0	4752.5	4752.5	0.0[c]
	1	5626.7	5626.7	0.0[c]

State	Fitted spectroscopic constants T_0 (cm^{-1})	ω_e (cm^{-1})	$\omega_e x_e$ (cm^{-1})
[4.75]	4752.5[c]	$\Delta G_{1/2}=874.2$ cm^{-1}[c]	
$[1.2]\,^3\Delta_2$	1188.66[c]	1002.66[c]	11.73[c]
$X\,^3\Delta_1$	0.0[b]	983.2±3.9	10.8±1.1

[a]Measured vibronic level energies were fitted to the formula $G_v=T_0+v\omega_e-(v^2+v)\omega_e x_e$, with T_0 constrained to be 0.0 for the $X\,^3\Delta_1$ state.
[b]Constrained to be zero in the fitting procedure.
[c]For the $[1.2]\,^3\Delta_2$ and [4.75] states, sufficient vibrational levels were observed for a unique determination of T_0, ω_e, and $\omega_e x_e$; and T_0 and $\Delta G_{1/2}$, respectively. Because these parameters were not overdetermined, no error estimates could be provided.

2. The $X^3\Delta_1$ state

Vibrational levels $v''=0$, 1, 2, and 3 of the $X\,^3\Delta_1$ ground state were observed in all but three of the dispersed fluorescence spectra that were collected. Each vibrational feature of sufficient intensity was recorded using a high-resolution diffraction grating to obtain an interpretable rotational contour. As displayed in Fig. 3, emission to the $v''=0$ level of the $X\,^3\Delta_1$ ground state following excitation of the 0-0 band of the $[17.6]2\leftarrow X\,^3\Delta_1$ system results in an intense *Q* branch and an *R* branch of greater intensity than the *P* branch, as expected from the Hönl–London formulas for this $\Omega'=2\rightarrow\Omega''=1$ emission.[68] The measured energies of the $v''=0$, 1, 2, and 3 vibrational levels were fitted to the form of Eq. (3.6), with T_0 constrained to be zero. The resulting values of the ground-state vibrational constants were $\omega_e=983.2(3.9)$ cm^{-1} and $\omega_e x_e=10.8(1.1)$ cm^{-1}.

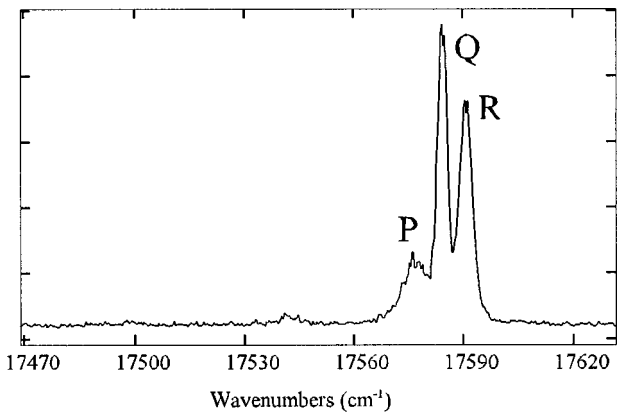

FIG. 3. Dispersed fluorescence spectrum of the $[17.6]2\rightarrow X\,^3\Delta_1$ 0-0 band. The strong *R* and *Q* branches and much weaker *P* branch are indicative of an emission process in which Ω decreases by 1.

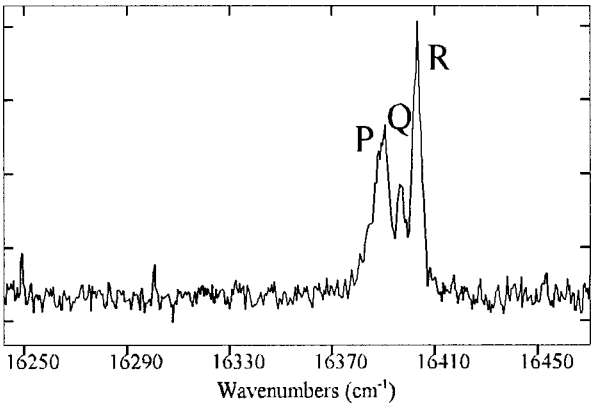

FIG. 4. Dispersed fluorescence spectrum of the $[17.6]2 \rightarrow [1.2]\,^3\Delta_2$ 0-0 band. The similar intensities of the *R* and *P* branches, in combination with the weak intensity of the *Q* branch, identifies this as a parallel band in which $\Delta\Omega = 0$.

3. The $[1.2]\,^3\Delta_2$ state

Fluorescence to the first low-lying excited electronic state was much less intense than fluorescence back to the $X\,^3\Delta_1$ ground state. Nevertheless, accurate measurements of the lower-state energies could be made by averaging the values obtained via different excitations. In addition, high-resolution dispersed fluorescence spectra allowed assignment of the Ω value for the state. As displayed in Fig. 4, the rotational contour of the 0-0 emission band, which occurs following excitation of the 0-0 band of the $[17.6]2 \leftarrow X\,^3\Delta_1$ system, reveals a weak *Q* branch, and strong *R* and *P* branches, which are of comparable intensity. This is consistent with a parallel transition in which $\Omega' = \Omega''$. Because the excitation band was previously investigated by R2PI spectroscopy and is known to have $\Omega' = 2$, this then implies that the lower state of this emission has $\Omega'' = 2$ as well. Both the photoelectron study and the theoretical investigation of WC concluded that the first excited electronic state of WC has the symmetry term $^3\Delta_2$.[30,57] These studies placed this level at 1226 ± 80 and 1656 cm^{-1}, respectively, in good agreement with our measurement of $T_0 = 1188.7\,cm^{-1}$. Accordingly, we assign this second emission band system to the $[1.2]\,^3\Delta_2$ state, which is the lowest excited spin–orbit component of the $X\,^3\Delta_1$ ground state. The measured vibrational levels allow the vibrational constants to be derived as $\omega_e = 1002.66\,cm^{-1}$ and $\omega_e x_e = 11.73\,cm^{-1}$.

4. The [4.75] state

The dispersed fluorescence study also revealed a feature repeated in three of the spectra that were collected using higher excitation energies. The lower state of this feature lies 4752.5 cm^{-1} above the ground state. Unfortunately, the intensity of this emission was too low to permit a spectrum to be recorded using the higher-resolution diffraction gratings, so the Ω value of this state cannot be determined from our experiments. Assuming that the observed feature corresponds to emission to the $v = 0$ level of a new electronic state, its energy may be compared to that of a state found using photoelectron spectroscopy by Wang and co-workers.[30] These authors assigned a state lying 4541 ± 80 cm^{-1} above the ground state as a $^1\Delta$ state deriving from the same electronic configuration as the ground $^3\Delta$ term. While our measured energy for this state differs from that obtained in the photoelectron study by 211 cm^{-1}, it is likely that both measurements correspond to the same state and that the error limit reported in the photoelectron study is somewhat underestimated. A second feature was also observed 5626.7 cm^{-1} above the ground state using one excitation, and we believe that this corresponds to the $v = 1$ level of this state. If so, this state is characterized by $T_0 = 4752.5\,cm^{-1}$ and $\Delta G_{1/2} = 874.2\,cm^{-1}$. While it is possible that this state could be primarily of $^1\Delta_2$ character, our inability to determine the Ω value makes such an assignment speculative at best. For this reason, we prefer to designate the state only by its energy as the [4.75] state of WC. Possible symmetry labels for this state are discussed in Sec. IV C below.

IV. DISCUSSION

A. The $X\,^3\Delta_1$ ground state

The photoelectron spectroscopic study by Wang and coworkers assigned the ground state of WC as $^3\Delta_1$, arising from the $14\sigma^2 8\pi^4 15\sigma^2 4\delta^1 16\sigma^1$ electronic configuration.[30] This assignment was confirmed in high-level calculations performed by Balasubramanian[57] and is consistent with the value of $\Omega'' = 1$ found in the present study.

The measured ground-state bond length of $r_0''(^{184}W^{12}C) = 1.7135(2)$ Å is similar to the bond length observed in $^{184}W^{12}CH$ of $r_0 = 1.736\,68$ Å.[60] It is also close to the $r_e = 1.727$ Å value recently calculated for this molecule.[57] The measured bond length of WC is a bit larger than the bond lengths found for IrC ($r_e = 1.683$ Å Refs. 17 and 18) and PtC ($r_e = 1.6767$ Å Refs. 19, 20, 22, and 34). This is a direct result of the contraction of the $5d$ and $6s$ orbitals as one moves to the right within the $5d$ period.

Using the dispersed fluorescence technique, the vibrational frequency of the $^3\Delta_1$ state has been measured to be $\omega_e' = 983.2(3.9)\,cm^{-1}$. This is in superb agreement with the theoretical investigation, in which the vibrational frequency was calculated to be 977 cm^{-1}.[57] The measured ground-state vibrational frequency of WC is somewhat smaller than the vibrational frequencies of the low-lying triplet states of the isovalent MoC molecule, which are 1008.3 cm^{-1} (for $X\,^3\Sigma_{0^+}^-$) and 1003 cm^{-1} (for $[4.0]\,^3\Delta_2$).[7] When expressed in terms of vibrational force constants, however, the values for WC (6.42 mdyn/Å for $X\,^3\Delta_1$) and MoC (6.40 mdyn/Å for $X\,^3\Sigma_{0^+}^-$; 6.34 mdyn/Å for $[4.0]\,^3\Delta_2$) are nearly identical. This attests to the similarity of the chemical bonding in these isovalent molecules.

Despite the similarity in vibrational force constants, the $14\sigma^2 8\pi^4 15\sigma^2 4\delta^1 16\sigma^1\,^3\Delta_1$ ground state of WC differs from the ground state determined for the isovalent MoC molecule. In MoC, the ground state is a $^3\Sigma_{0^+}^-$ term deriving from a $10\sigma^2 5\pi^4 11\sigma^2 2\delta^2$ electronic configuration.[6,72] This difference in the ground term arises from variations in the ground states of the metal atoms. Molybdenum has an atomic ground-state configuration of $4d^5 5s^1$, while atomic tungsten has a ground-state configuration of $5d^4 6s^2$.[73] Clearly, atomic tungsten favors occupation of the valence *s* orbital to a

higher degree than does molybdenum, and this atomic tendency is carried over into the metal carbide, where occupation of the valence *s*-based molecular orbital (12σ in MoC, 16σ in WC) is more favored for WC than for MoC.

This change in ground-state electronic configuration in moving from Mo to W or from MoC to WC is a result of the relativistic stabilization of the $6s$ orbital in the $5d$ series of transition metals. The relativistic stabilization of the $6s$ orbital makes the ionization energies of the $5d$ metals higher than those of the $4d$ metals, gives metallic gold its yellow luster, makes mercury a liquid at room temperature, and causes the mercurous ion, Hg^+, to dimerize to Hg_2^{2+} in solution.[74] In the transition-metal carbides, stabilization of the $6s$ atomic orbital carries over to the $6s$-like 16σ orbital, causing this orbital to be occupied in the WC ground state. The same stabilization of the $6s$-based 16σ orbital also occurs in IrC, which has a $14\sigma^2 8\pi^4 15\sigma^2 4\delta^3 16\sigma^2\,{}^2\Delta_i$ ground state,[33,56] in contrast to the $10\sigma^2 5\pi^4 11\sigma^2 2\delta^4 12\sigma^1\,{}^2\Sigma^+$ ground state[14,15,32,75,76] of RhC and the $7\sigma^2 3\pi^4 8\sigma^2 1\delta^4 9\sigma^1\,{}^2\Sigma^+$ ground state[25,26] of CoC.

B. The [1.2] $^3\Delta_2$ low-lying excited state

The $[1.2]\,{}^3\Delta_2$ state found in the dispersed fluorescence study was found to have $T_0 = 1189\,\mathrm{cm}^{-1}$, $\omega_e = 1002.66\,\mathrm{cm}^{-1}$, and $\omega_e x_e = 11.73\,\mathrm{cm}^{-1}$. In the photoelectron study, Wang and co-workers found $T_0 = 1226(80)\,\mathrm{cm}^{-1}$, in good agreement with our result.[30] Unfortunately, the lack of a vibrational progression prevented these authors from measuring the vibrational constants for this state. In contrast, the one theoretical investigation reported to date predicted the $^3\Delta_2$ state to lie at 1656 cm^{-1}, substantially above the measured energy.[57]

A first-order perturbation treatment of the spin–orbit interactions in the $14\sigma^2 8\pi^4 15\sigma^2 4\delta^1 16\sigma^1\,{}^3\Delta$ state of WC predicts that the $\Omega = 1$, 2, and 3 substates will be equally spaced, with separations between sequential states given by a_δ.[77] Furthermore, assuming that the 4δ molecular orbital is unchanged from its $5d$ atomic parent, a_δ is exactly equal to the atomic spin–orbit parameter $\zeta_{5d}(\mathrm{W})$.[77] Values of this parameter may be computed using numerical Hartree–Fock methods developed by Froese Fischer,[78] providing values of $\zeta_{5d}(\mathrm{W}) = 2436.5\,\mathrm{cm}^{-1}$ (for the $6s^2 4d^4\,{}^5D$ ground state), 2155.1 cm^{-1} (for the $6s^1 4d^5\,{}^7S$ term), and 1929.1 cm^{-1} (for the $6s^0 4d^6\,{}^5D$ term). Allowing for the possibility that the tungsten atom may carry a substantial partial positive charge in WC, it is possible that more appropriate values of $\zeta_{5d}(\mathrm{W})$ may be given by calculations on the W^+ cation. These give $\zeta_{5d}(\mathrm{W}) = 2735.9\,\mathrm{cm}^{-1}$ (for the $6s^2 5d^3\,{}^4F$ term), 2463.6 cm^{-1} (for the $6s^1 5d^4\,{}^6D$ term), and 2272.6 cm^{-1} (for the $6s^0 5d^5\,{}^6S$ term). Based on these results, we can expect that $\zeta_{5d}(\mathrm{W})$ probably lies in the range of 2100–2500 cm^{-1} for WC, because in this molecule the 16σ orbital, which is primarily $6s$ in character, is singly occupied. Thus, the $6s^1 4d^5\,{}^7S$ term of W and the $6s^1 5d^4\,{}^6D$ term of W^+ are the most appropriate comparisons.

The measured separation between the $X\,{}^3\Delta_1$ ground state and the $[1.2]\,{}^3\Delta_2$ first excited state, 1189 cm^{-1}, is much smaller than the separation predicted using the range of ζ values mentioned above. This indicates that there are significant off-diagonal spin–orbit interactions in this system. The most important of these is the interaction between the $14\sigma^2 8\pi^4 15\sigma^2 4\delta^1 16\sigma^1\,{}^3\Delta_2$ state and the $^1\Delta_2$ state that derives from this same configuration. This interaction pushes the $^3\Delta_2$ state to lower energies and also leads to substantial singlet–triplet mixing in the states that are nominally described as $^3\Delta_2$ and $^1\Delta_2$. This phenomenon may be understood by considering the matrix Hamiltonian for the $^3\Delta_1$, $^3\Delta_3$, $^3\Delta_2$, and $^1\Delta_2$ states:

$$\underline{\underline{H}} = \begin{array}{c} \begin{matrix} |^3\Delta_1\rangle & |^3\Delta_2\rangle & |^1\Delta_2\rangle & |^3\Delta_3\rangle \end{matrix} \\ \begin{pmatrix} T_3 - a_\delta & 0 & 0 & 0 \\ 0 & T_3 & -a_\delta & 0 \\ 0 & -a_\delta & T_1 & 0 \\ 0 & 0 & 0 & T_3 + a_\delta \end{pmatrix} \end{array}. \tag{4.1}$$

This Hamiltonian has the energy eigenvalues

$$E(^3\Delta_1) = T_3 - a_\delta, \quad E(^3\Delta_3) = T_3 + a_\delta,$$

$$E(^3\Delta_2) = \tfrac{1}{2}\{T_1 + T_3 - [(T_1 - T_3)^2 + 4a_\delta^2]^{1/2}\},$$

$$E(^1\Delta_2) = \tfrac{1}{2}\{T_1 + T_3 + [(T_1 - T_3)^2 + 4a_\delta^2]^{1/2}\}.$$

Setting these energies equal to the measured energies of $E(^3\Delta_1) = 0\,\mathrm{cm}^{-1}$ and $E(^3\Delta_2) = 1189\,\mathrm{cm}^{-1}$, and assuming a value of a_δ, it is possible to solve for the values of T_1, T_3, $E(^3\Delta_3)$, and $E(^1\Delta_2)$. For values of a_δ in the expected range of 2100–2500 cm^{-1}, the $^1\Delta_2$ state is predicted to lie at an energy of 6940–7270 cm^{-1}. Likewise, the $^3\Delta_3$ state is predicted to lie at an energy of 4200–5000 cm^{-1}.

C. The [4.75] state of WC

The least well-characterized electronic state of WC reported in this work is the [4.75] state, for which $T_0 = 4752.5\,\mathrm{cm}^{-1}$ and $\Delta G_{1/2} = 874.2\,\mathrm{cm}^{-1}$. Our first thought was that this state was the $^1\Delta_2$ state deriving from the same $14\sigma^2 8\pi^4 15\sigma^2 4\delta^1 16\sigma^1$ configuration that generates the $^3\Delta_1$ ground state. In fact, this assignment was suggested for a state located at 4541 cm^{-1} in the photoelectron spectroscopy experiments.[30] The calculations presented in the previous paragraph, however, rule out this possibility unless there are large additional spin–orbit perturbations that affect either the $^3\Delta_2$ or $^1\Delta_2$ states. For a molecule containing atoms with valence orbitals for which ζ is as large as 2000 cm^{-1}, such perturbations are certainly possible.

Another possible assignment for the [4.75] state is the $^3\Delta_3$ excited spin–orbit component of the ground electronic state. As mentioned in the previous section, this state is expected to lie in the range 4200–5000 cm^{-1}, in agreement with the measured value of $T_0 = 4752.5\,\mathrm{cm}^{-1}$. In the theoretical calculation of WC, the $^3\Delta_3$ state is predicted to lie at 4394 cm^{-1}.[57] Based on the agreement between the calculated energy of the $^3\Delta_3$ state and the state measured in the photoelectron experiments to lie at 4541 cm^{-1}, the theoretical investigation reassigned this state from $^1\Delta_2$ to $^3\Delta_3$.[57] We believe that our [4.75] state, which lies at $T_0 = 4752.5\,\mathrm{cm}^{-1}$, is the same state that was measured in the photoelectron study to lie at 4541 cm^{-1}. While this certainly could be a $^3\Delta_3$ state,

this assignment requires that the $\Delta\Sigma=0$ selection rule be broken in either the excitation or emission step of our dispersed fluorescence study, or both. Excitation from the $^3\Delta_1$ ($\Sigma=-1$) ground state to an excited state with $\Omega=2$ followed by emission to the $^3\Delta_3$ ($\Sigma=+1$) state requires that Σ change by 2 units in a two-photon process. In molecules with small spin–orbit interactions, such a process would be impossible to observe. While it is conceivable that it could occur in WC, this process requires considerable spin–orbit mixing. For example, if both the $^3\Delta_1$ initial state and the $^3\Delta_3$ final state have well-defined values of S, Λ, and Σ, then such a process would require that the $\Omega=2$ excited state have significant $^3\Phi_2$ character (to make the excitation from the $^3\Delta_1$ state allowed) along with significant $^3\Pi_2$ character (to make the emission to the $^3\Delta_3$ state allowed). The spin–orbit operator, however, cannot directly mix a $^3\Phi_2$ state with a $^3\Pi_2$ state because it can only couple states that differ in Λ by ±1 or 0.[77] Thus, the excited state would also have to have some $\Lambda=2$ character as well, and this would have to be mixed with both the $^3\Phi_2(\Lambda=3)$ and $^3\Pi_2(\Lambda=1)$ states. Thus, two separate off-diagonal spin–orbit interactions would be required to account for the observation of fluorescence to a $^3\Delta_3$ state. Although possible, this seems rather improbable.

Finally, we may examine the other electronic states that are calculated to lie near 4752 cm^{-1}, in the hope of identifying a more likely candidate. Because our state was detected via fluorescence from an $\Omega=2$ state, we can be confident that its Ω value is 1, 2, or 3. Calculated states lying within 2000 cm^{-1} of our measured T_0 that satisfy this constraint are a $^5\Sigma^-(1)$ state at 3350 cm^{-1}, a $^5\Sigma^-(2)$ state at 3690 cm^{-1}, the previously discussed $^3\Delta_3$ state at 4394 cm^{-1}, a $^5\Pi_2$ state at 5268 cm^{-1}, a $^3\Sigma^-(1)$ state at 5306 cm^{-1}, a $^5\Pi_3$ state at 5373 cm^{-1}, a $^3\Delta_1$ state at 6055 cm^{-1}, a $^3\Delta_2-{}^1\Delta_2$ mixed state at 6227 cm^{-1}, and a $^5\Pi_1$ state at 6693 cm^{-1}.[57] Of these possibilities, the $^5\Sigma^-(1)$, $^5\Sigma^-(2)$, $^3\Sigma^-(1)$, or $^5\Pi_3$ states seem unlikely to be observed, since these also require at least two separate off-diagonal spin–orbit interactions for their observation. Fluorescence to the $^3\Delta_1$ state calculated at 6055 cm^{-1}, however, is just as allowed on the basis of S, Λ, and Σ as fluorescence back to the $^3\Delta_1$ ground state. Furthermore, the calculated vibrational frequency of this state is 851.5 cm^{-1},[57] in rather good agreement with our measured value of $\Delta G_{1/2}=874.2\,cm^{-1}$. The last two possibilities for the [4.75] state are the $^3\Delta_2-{}^1\Delta_2$ mixed state calculated at 6227 cm^{-1} and the $^5\Pi_1$ state calculated at 6693 cm^{-1}.[57] Fluorescence to either of these states could be induced by a single off-diagonal spin–orbit interaction in the $\Omega=2$ state that was excited, making these likely possibilities as well. The $^5\Pi$ state is calculated to have a vibrational frequency of 885 cm^{-1},[57] also in rather good agreement with our measured value of $\Delta G_{1/2}$.

On the basis of these spin–orbit considerations, it seems most likely that the [4.75] state of WC is the first excited state of $^3\Delta_1$ symmetry, the $^3\Delta_2-{}^1\Delta_2$ mixed state, or the $^5\Pi_1$ state. Further experiments or theoretical calculations will obviously be required to sort these possibilities out further.

D. The [17.6]2 state

The photoelectron study of WC observed an excited state at $17\,535\pm160$ cm^{-1} and assigned this as the $14\sigma^2 8\pi^3 15\sigma^2 4\delta^1 16\sigma^2\,{}^3\Phi_2$ state.[30] The theoretical investigation predicted a $^1\Gamma$ excited state near 17 767 cm^{-1} and on this basis reassigned the 17 535 cm^{-1} state observed in the photoelectron work as $^1\Gamma$.[57] In the present study, an excited $\Omega=2$ state is observed by resonant two-photon ionization spectroscopy at 17 585 cm^{-1}. It is most likely that this is the same state as that found in the photoelectron study at 17 535 ±160 cm^{-1}. Furthermore, if we assume that the ground state is of nearly pure $^3\Delta_1$ character, then this $\Omega=2$ excited state gains its oscillator strength for transitions with the ground state through $^3\Phi_2$ character that is present in the excited-state wave function. This is true because the only Hund's case (a) allowed transition between a $^3\Delta_1$ state and an $\Omega=2$ state is to a $^3\Phi_2$ state. Thus, we are tempted to assign the [17.6]2 state as $^3\Phi_2$. In any case, whatever the dominant Hund's case (a) character of the [17.6]2 state may be, our identification of its $\Omega=2$ value implies that it cannot be the $^1\Gamma$ state that was proposed in the theoretical investigation. A $^1\Gamma$ state only generates a single Ω state, with $\Omega=4$.

In the theoretical investigation of WC, the only $\Omega=2$ states calculated within 5000 cm^{-1} of the [17.6]2 state are strongly mixed states at 12 800 and 15 613 cm^{-1}.[57] The latter of these two states is identified as having 36% $^1\Delta_2$ character, 24% $^5\Pi_2$ character, 17% $^3\Delta_2$ character, and 10% $^1\Delta_2$ character from a second $^1\Delta_2$ state.[57] The lack of reported $^3\Phi_2$ character in this wave function suggests that it is not the state we have observed. For the remaining calculated $\Omega=2$ state, which was predicted to lie at 12 800 cm^{-1}, almost no details concerning its Hund's case (a) character, its bond length, or vibrational frequency were provided. Therefore, it is impossible for us to make a comparison to the theoretical results at this time.

V. CONCLUSION

In this spectroscopic study of WC, 15 discrete bands were found and 9 of these features were rotationally resolved. The ground-state molecular term was confirmed as $^3\Delta_1$, with a bond length of $r_0''(^{184}W^{12}C)=1.7135(2)$ Å, a vibrational frequency of $\omega_e'=983.2(3.9)\,cm^{-1}$, and an anharmonicity of $\omega_e x_e=10.8\,cm^{-1}$. The spin–orbit excited $^3\Delta_2$ state was observed by dispersed fluorescence spectroscopy at $T_0=1188.7\,cm^{-1}$ with $\omega_e=1002.7\,cm^{-1}$ and $\omega_e x_e=11.7\,cm^{-1}$. A second low-lying excited state was observed by dispersed fluorescence spectroscopy at $T_0=4752\,cm^{-1}$, with $\Delta G_{1/2}=874\,cm^{-1}$. Finally, a vibrational progression was observed by R2PI spectroscopy beginning at 17 585 cm^{-1}, with $\omega_e'(^{184}W^{12}C)=752.56(4.88)\,cm^{-1}$ and $r_e'(^{184}W^{12}C)=1.747(4)$ Å. The upper state of this band system has $\Omega=2$ and is identified for future reference as the [17.6]2 state. It derives its absorption intensity from a $^3\Phi_2$ Hund's case (a) basis function, which may be the major Hund's case (a) contributor to this state.

ACKNOWLEDGMENTS

The authors thank the Department of Energy for support for this work, under Grant No. DE-FG03-01ER15176. A.W.S. was funded by an Undergraduate Research Opportunities Program (UROP) Grant provided by the University of Utah. We greatly appreciate the generous gift of a fused silica cell containing isotopically pure ^{130}Te from Tim Steimle, which greatly facilitated the calibration of the transitions above 20 000 cm^{-1}. The authors also thank Jason Christofferson for the development of a combination difference software routine that aided in the analysis of the overlapping bands, and Marc Airola for help in setting up the dispersed fluorescence experiments.

[1] G. W. Parshall and S. D. Ittel, *Homogeneous Catalysis: The Applications and Chemistry of Catalysis by Soluble Transition Metal Complexes*, 2nd ed. (Wiley, New York, 1992).
[2] B. M. Trost and M. Lautens, J. Am. Chem. Soc. **104**, 5543 (1982).
[3] B. M. Trost and M.-H. Hung, J. Am. Chem. Soc. **105**, 7757 (1983).
[4] B. M. Trost and M. Lautens, J. Am. Chem. Soc. **105**, 3343 (1983).
[5] D. J. Brugh and M. D. Morse, J. Chem. Phys. **107**, 9772 (1997).
[6] D. J. Brugh, T. J. Ronningen, and M. D. Morse, J. Chem. Phys. **109**, 7851 (1998).
[7] R. S. DaBell, R. G. Meyer, and M. D. Morse, J. Chem. Phys. **114**, 2938 (2001).
[8] J. D. Langenberg, R. S. DaBell, L. Shao, D. Dreessen, and M. D. Morse, J. Chem. Phys. **109**, 7863 (1998).
[9] J. D. Langenberg, L. Shao, and M. D. Morse, J. Chem. Phys. **111**, 4077 (1999).
[10] R. Scullman and B. Thelin, Phys. Scr. **3**, 19 (1971).
[11] R. Scullman and B. Thelin, Phys. Scr. **5**, 201 (1972).
[12] N. S. McIntyre, A. Vander Auwera-Mahieu, and J. Drowart, Trans. Faraday Soc. **64**, 3006 (1968).
[13] A. Lagerqvist, H. Neuhaus, and R. Scullman, Z. Naturforsch. A **20a**, 751 (1965).
[14] A. Lagerqvist and R. Scullman, Ark. Fys. **32**, 475 (1966).
[15] B. Kaving and R. Scullman, J. Mol. Spectrosc. **32**, 475 (1969).
[16] A. V. Auwera-Mahieu and J. Drowart, Chem. Phys. Lett. **1**, 311 (1967).
[17] K. Jansson, R. Scullman, and B. Yttermo, Chem. Phys. Lett. **4**, 188 (1969).
[18] K. Jansson and R. Scullman, J. Mol. Spectrosc. **36**, 248 (1970).
[19] O. Appelblad, C. Nilsson, and R. Scullman, Phys. Scr. **7**, 65 (1973).
[20] R. Scullman and B. Yttermo, Ark. Fys. **33**, 231 (1966).
[21] H. Neuhaus, R. Scullman, and B. Yttermo, Z. Naturforsch. A **20a**, 162 (1965).
[22] O. Appelblad, R. F. Barrow, and R. Scullman, Proc. Phys. Soc. London **91**, 260 (1967).
[23] W. J. Balfour, J. Cao, C. V. V. Prasad, and C. X. Qian, J. Chem. Phys. **103**, 4046 (1995).
[24] K. Aiuchi, K. Tsuji, and K. Shibuya, Chem. Phys. Lett. **309**, 229 (1999).
[25] M. Barnes, A. J. Merer, and G. F. Metha, J. Chem. Phys. **103**, 8360 (1995).
[26] A. G. Adam and J. R. D. Peers, J. Mol. Spectrosc. **181**, 24 (1997).
[27] B. Simard, P. A. Hackett, and W. J. Balfour, Chem. Phys. Lett. **230**, 103 (1994).
[28] A. J. Merer and J. R. D. Peers, in Ohio State 53rd International Symposium on Molecular Spectroscopy, Columbus, OH, 1998, Abstract R104, p. 249.
[29] B. Simard, P. I. Presunka, H. P. Loock, A. Bérces, and O. Launila, J. Chem. Phys. **107**, 307 (1997).
[30] X. Li, S. S. Liu, W. Chen, and L.-S. Wang, J. Chem. Phys. **111**, 2464 (1999).
[31] X. Li and L.-S. Wang, J. Chem. Phys. **109**, 5264 (1998).
[32] W. J. Balfour, S. G. Fougère, R. F. Heuff, C. X. W. Qian, and C. Zhou, J. Mol. Spectrosc. **198**, 393 (1999).
[33] A. J. Marr, M. E. Flores, and T. C. Steimle, J. Chem. Phys. **104**, 8183 (1996).
[34] T. C. Steimle, K. Y. Jung, and B.-Z. Li, J. Chem. Phys. **102**, 5937 (1995).
[35] T. C. Steimle, K. Y. Jung, and B.-Z. Li, J. Chem. Phys. **103**, 1767 (1995).
[36] S. A. Beaton and T. C. Steimle, J. Chem. Phys. **111**, 10876 (1999).
[37] T. C. Steimle, M. L. Costen, G. E. Hall, and T. J. Sears, Chem. Phys. Lett. **319**, 363 (2000).
[38] J. Cao, Ph.D. thesis, University of Victoria (1997).
[39] M. D. Allen, T. C. Pesch, and L. M. Ziurys, Astrophys. J. Lett. **472**, L57 (1996).
[40] R. J. Van Zee, J. J. Bianchini, and W. Weltner, Jr., Chem. Phys. Lett. **127**, 314 (1986).
[41] D. J. Brugh and M. D. Morse (unpublished).
[42] R. S. DaBell, S. M. Sickafoose, and M. D. Morse (unpublished).
[43] Y. M. Hamrick and W. Weltner, Jr., J. Chem. Phys. **94**, 3371 (1991).
[44] C. W. Bauschlicher, Jr. and P. E. M. Siegbahn, Chem. Phys. Lett. **104**, 331 (1984).
[45] S. Sokolova and A. Lüchow, Chem. Phys. Lett. **320**, 421 (2000).
[46] M. D. Hack, R. G. A. R. Maclagan, G. E. Scuseria, and M. S. Gordon, J. Chem. Phys. **104**, 6628 (1996).
[47] R. G. A. R. Maclagan and G. E. Scuseria, Chem. Phys. Lett. **262**, 87 (1996).
[48] S. M. Mattar, J. Phys. Chem. **97**, 3171 (1993).
[49] I. Shim and K. A. Gingerich, Int. J. Quantum Chem. **42**, 349 (1992).
[50] R. G. A. R. Maclagan and G. E. Scuseria, J. Chem. Phys. **106**, 1491 (1997).
[51] I. Shim and K. A. Gingerich, Eur. Phys. J. D **7**, 163 (1999).
[52] I. Shim and K. A. Gingerich, Z. Phys. D: At., Mol. Clusters **12**, 373 (1989).
[53] I. Shim and K. A. Gingerich, Chem. Phys. Lett. **303**, 87 (1999).
[54] S. K. Gupta, B. M. Nappi, and K. A. Gingerich, J. Phys. Chem. **85**, 971 (1981).
[55] D. Majumdar and K. Balasubramanian, Chem. Phys. Lett. **284**, 273 (1998).
[56] H. Tan, M. Liao, and K. Balasubramanian, Chem. Phys. Lett. **280**, 219 (1997).
[57] K. Balasubramanian, J. Chem. Phys. **112**, 7425 (2000).
[58] L. Andrews and M. Zhou, J. Phys. Chem. A **103**, 4167 (1999).
[59] R. S. Ram and P. F. Bernath, J. Opt. Soc. Am. B **11**, 225 (1994).
[60] M. Barnes, D. A. Gillett, A. J. Merer, and G. F. Metha, J. Chem. Phys. **105**, 6168 (1996).
[61] Z. Fu, G. W. Lemire, Y. M. Hamrick, S. Taylor, J.-C. Shui, and M. D. Morse, J. Chem. Phys. **88**, 3524 (1988).
[62] G. W. Lemire, G. A. Bishea, S. A. Heidecke, and M. D. Morse, J. Chem. Phys. **92**, 121 (1990).
[63] W. C. Wiley and I. H. McLaren, Rev. Sci. Instrum. **26**, 1150 (1955).
[64] V. I. Karataev, B. A. Mamyrin, and D. V. Shmikk, Zh. Tekh. Fitz. **41**, 1498, (1971) [Zh. Tekh. Fiz. **16**, 1177 (1972)].
[65] S. Gerstenkorn and P. Luc, *Atlas du Spectre d'Absorption de la Molecule d'Iode entre 14,800–20,000 cm^{-1}* (CNRS, Paris, 1978).
[66] J. Cariou and P. Luc, *Atlas du Spectre d'Absorption de la Molécule de Tellure entre 18,500–23,800 cm^{-1}* (CNRS, Paris, 1980).
[67] F. M. Phelps, *Massachusetts Institute of Technology Wavelength Tables* (MIT Press, Cambridge, MA, 1969).
[68] G. Herzberg, *Molecular Spectra and Molecular Structure. I. Spectra of Diatomic Molecules*, 2nd ed. (Van Nostrand Reinhold, New York, 1950).
[69] See EPAPS Document No. E-JCPSA6-116-013203 for 19 pages of absolute line positions and rotational fits. This document may be retrieved via the EPAPS homepage (http://www.aip.org/pubservs/epaps.html) or from ftp.aip.org in the directory /epaps/. See the EPAPS homepage for more information.
[70] A. G. Adam, Y. Azuma, J. A. Barry, G. Huang, M. P. J. Lyne, A. J. Merer, and J. O. Schröder, J. Chem. Phys. **86**, 5231 (1987).
[71] P. F. Bernath, *Spectra of Atoms and Molecules* (Oxford University Press, New York, 1995).
[72] I. Shim and K. A. Gingerich, J. Chem. Phys. **106**, 8093 (1997).
[73] C. E. Moore, *Atomic Energy Levels*, Natl. Bur. Stand. U.S. Circ. No. 467 (U.S. Government Printing Office, Washington, D.C., 1971).
[74] K. Balasubramanian, J. Chem. Phys. **93**, 6585 (1989).
[75] J. M. Brom, Jr., W. R. M. Graham, and W. Weltner, Jr., J. Chem. Phys. **57**, 4116 (1972).
[76] H. Tan, M. Liao, and K. Balasubramanian, Chem. Phys. Lett. **280**, 423 (1997).
[77] H. Lefebvre-Brion and R. W. Field, *Perturbations in the Spectra of Diatomic Molecules*, 1st ed. (Academic, Orlando, 1986).
[78] C. F. Fischer, *The Hartree-Fock Method for Atoms* (Wiley, New York, 1977).